

# NJC

Accepted Manuscript



This is an *Accepted Manuscript*, which has been through the Royal Society of Chemistry peer review process and has been accepted for publication.

*Accepted Manuscripts* are published online shortly after acceptance, before technical editing, formatting and proof reading. Using this free service, authors can make their results available to the community, in citable form, before we publish the edited article. We will replace this *Accepted Manuscript* with the edited and formatted *Advance Article* as soon as it is available.

You can find more information about *Accepted Manuscripts* in the [Information for Authors](#).

Please note that technical editing may introduce minor changes to the text and/or graphics, which may alter content. The journal's standard [Terms & Conditions](#) and the [Ethical guidelines](#) still apply. In no event shall the Royal Society of Chemistry be held responsible for any errors or omissions in this *Accepted Manuscript* or any consequences arising from the use of any information it contains.

**Folate-PEG functionalized silica CdTe quantum dots as fluorescent probes for cancer cell imaging†**

Miao Lu<sup>a</sup>, Wendian Zhang<sup>a</sup>, Yongkang Gai<sup>a</sup>, Tan Yang<sup>a</sup>, Peng Ye<sup>b</sup>, Guang Yang<sup>c</sup>, Xiang Ma<sup>a,\*</sup> and Guangya Xiang<sup>a,\*</sup>

<sup>a</sup> School of Pharmacy, Tongji Medical College, Huazhong University of Science and Technology, Wuhan 430030, Hubei, People's Republic of China.

<sup>b</sup> Department of Pharmacy, Wuhan University, Renmin Hospital, Wuhan 430060, Hubei Province, People's Republic of China.

<sup>c</sup> School of Medicine, Jiangnan University, Wuhan, Hubei, 430030, China

\*Corresponding Author:

E-Mails: [gyxiang1968@hotmail.com](mailto:gyxiang1968@hotmail.com) (G.X); [maxwellcn@yahoo.com](mailto:maxwellcn@yahoo.com) (X.M). Tel.:

[+86-27-8369-2793](tel:+86-27-8369-2793) (G.-Y.X. and X.M.); Fax: [+86-27-8369-2762](tel:+86-27-8369-2762) (G.-Y.X. and X.M.).

† Electronic supplementary information (ESI) available

**Abstract**

Fluorescent probes based on quantum dots (QDs) are emerging as ideal tools for sensing and imaging in biological applications owing to their great advantages such as high sensitivity and unique optical properties. Using QDs as a potential effective tool for tumor optical imaging would allow early diagnosis, monitoring tumor progression and treatment efficiency. We prepared a novel folate receptor-targeted, PEG-modified fluorescent probe based on silica-coated CdTe QDs. In the study, the hydrophilic thioglycolic acid stabilized CdTe QDs were directly synthesized in water phase; the water-in-oil (W/O) reverse microemulsion method was applied to prepare the highly fluorescent amino-functionalized core-shell CdTe@SiO<sub>2</sub> particles; subsequently, polyethylene glycol (PEG) and folate molecules were successfully bioconjugated with the CdTe@SiO<sub>2</sub> particles through the amino groups. The as-performed particles were characterized by UV-Vis absorption, fluorescence measurements, particle size, zeta potential and high-resolution transmission electron microscopy (HR-TEM). The bioimaging efficiency and specificity of the prepared fluorescent probes were further evaluated on KB cells. Results indicate that the silica film encapsulated and PEGylated CdTe QDs can significantly reduce the cytotoxicity of CdTe QDs. In conclusion, folate receptor-targeted, PEG-modified and silica-coated CdTe quantum dots fluorescent probes are highly promising for tumor imaging in the near future.

**Keywords**

fluorescent probes; nanoparticles; folate targeting; quantum dots; KB cells

## INTRODUCTION

Cancer is the leading cause of death in economically developed countries and the second leading cause of death in developing countries<sup>1</sup>. While significant progress has been made in dropping cancer mortality rates, the number of new cancer cases continues to climb. Increasing incidence of cancer leads to a greater demand for advancements in early cancer diagnostics, treatment and ongoing monitoring. Recent development has witnessed that molecular imaging plays an expanding role in the management of the above increased demands<sup>2-5</sup>. Fluorescence-based diagnostic imaging techniques are promising in the cancer diagnostics and treatment monitoring due to their advantage of high sensitivity and rapid response, compared to the currently clinical available imaging techniques such as X-ray computed tomography (CT) and magnetic resonance imaging (MRI)<sup>6,7</sup>. With the advancement of cancer nanotechnology, tremendous effort has been put forth to design and develop methods to fabricate nanotools onto novel fluorescent probes<sup>8,9</sup>. Fluorescent nanoparticle based probes in certain size range have a strong tendency to enter and retain in solid tumor tissue with enhanced permeation and retention (EPR) effect, advancing their use for in vivo tumor imaging<sup>10</sup>. Furthermore, large surface area and their surface structure offer a platform for designing and fabricating multimodal/multifunctional nanoparticles<sup>10</sup>.

Quantum dots (QDs) represented one of the most rapidly advancing fluorescent imaging probes benefiting from their unique optical properties. Advantages of ODs over other fluorescent dyes included their excellent optical properties such as high

brightness, broad absorption spectra, narrow, symmetric and size-tunable emission spectra and superior photostability<sup>8, 10, 11</sup>. The most studied and applied QDs were made of elements from the II and VI groups (e.g. CdSe, PbSe, CdS, and ZnO) of periodic table of elements. The QDs were primarily prepared *via* hot injection organometallic route and aqueous synthesis approaches. The organometallic route synthesized QDs with excellent optical properties; however, such organic synthesized QDs were of hydrophobic nature and not readily soluble, thus cannot be directly used in bioapplications<sup>12, 13</sup>. On the other hand, aqueous synthesized QDs were directly used for biological applications without any post-treatment, and the synthetic processes were cheaper, less toxic, simpler, more reproducible and environmentally friendly than the organometallic routes were<sup>14, 15</sup>. Nevertheless, the cytotoxicity as a result of heavy metal ions release, as well as chemical and colloidal instabilities of QDs limited their biological applications<sup>16</sup>. To solve the cytotoxicity and instability problem, QDs were often coated with inert materials such as silica as a shell<sup>17</sup>. The silica shell platform also allowed manipulation *via* standard silane coupling chemistry<sup>17</sup>.

The encapsulation of inorganic QDs nanoparticles with silica shells has been widely investigated<sup>18, 19</sup>. Generally, there were two typical established methods for preparing silica-coated QDs<sup>18, 20</sup>. Using the coating method developed by W. Stöber<sup>20</sup>, the starting QDs material must be able to occur surface exchange with silane agent, such as 3-mercaptopropyl trimethoxysilane (MPS). The needed multiple modification steps made the size distribution of the prepared QDs@silica nanoparticles with broad

range from 30 to 150 nm<sup>19</sup>. Using the reverse microemulsion approach developed by Chang et. al<sup>21</sup>, QDs were successfully encapsulated in silica nanoparticles to yield more uniformed sphere in the size range of 30-150 nm. In comparison with the Stöber method, the obvious advantages of the microemulsion approach also included the robust reaction conditions, the smooth surfaces of the resulting nanoparticles and the narrow size distributions<sup>22</sup>.

Polyethyleneglycol (PEG) was considered to be the best biocompatible material which is well known to increase the circulation time by decreasing the clearance of the nanoparticles via reticuloendothelial system (RES)<sup>23</sup>. Conjugated with PEG moieties, the modified ODs could be highly biocompatible without any loss in fluorescence intensity of original QDs. In addition, the PEG-QD conjugates are also suitable for biofunctionalization due to the highly reactive functional groups. In conjugation with targeting moieties, such as small molecules, antibodies, aptamers, peptides etc, the functionalized ODs were successfully used for cancer cells targeting with high specificity<sup>7, 24-28</sup>. Therefore, considering the excellent luminescent properties of cadmium based QDs and their cytotoxicity, low biocompatibility and non-specificity, we hypothesized that folate-PEG functionalized silica CdTe QDs as fluorescent probes would be a promising diagnostic approach for tumor imaging.

Therefore, in this study, we prepared the silica coated aqueous CdTe QDs. The resulted coated QDs were further pegylated and functionalized with folate. The UV-Vis absorption, fluorescence measurements, particle size, zeta potential and high-resolution transmission electron microscopy (HR-TEM) were used to

characterize the physical and chemical properties of the nanoparticles. In addition, we also investigated the stability of the nanoparticles for several months. MTT assays against the folate receptor high expressed human nasopharyngeal carcinoma cells (KB) were performed to evaluate the cytotoxicity. Furthermore, the bioimaging efficiency and specificity of the prepared fluorescent probes were also studied using KB cell uptake assay. Thus, here we report the preparation of highly biocompatible folate receptor-targeted, PEG-modified and silica-coated CdTe quantum dots as fluorescent probes and application of them in cancer cell imaging by folate targeting scheme.

## RESULTS AND DISCUSSION

### Preparation and Characterizations

TGA-stabilized CdTe QDs were synthesized via an aqueous synthetic approach. The cadmium-TGA complex and NaHTe were mixed at room temperature and the mixture was refluxed under N<sub>2</sub> atmosphere. UV-visible absorption spectra and fluorescence emission spectra of the forming of TGA-stabilized CdTe QDs at different refluxing times was recorded under ultraviolet irradiation as shown in **Fig 1**. With the progress of the refluxing reaction, the fluorescent color changed from green to orange, and a red shift in both absorption and emission wavelengths were observed. This observation could be explained that the degree of polymerization between CdTe molecules increased as the reaction was going, making the particle size of nanoparticles gradually increased. When the quantum dot size increased to a certain value, the quantum size effect was becoming significant. The quantum size effects

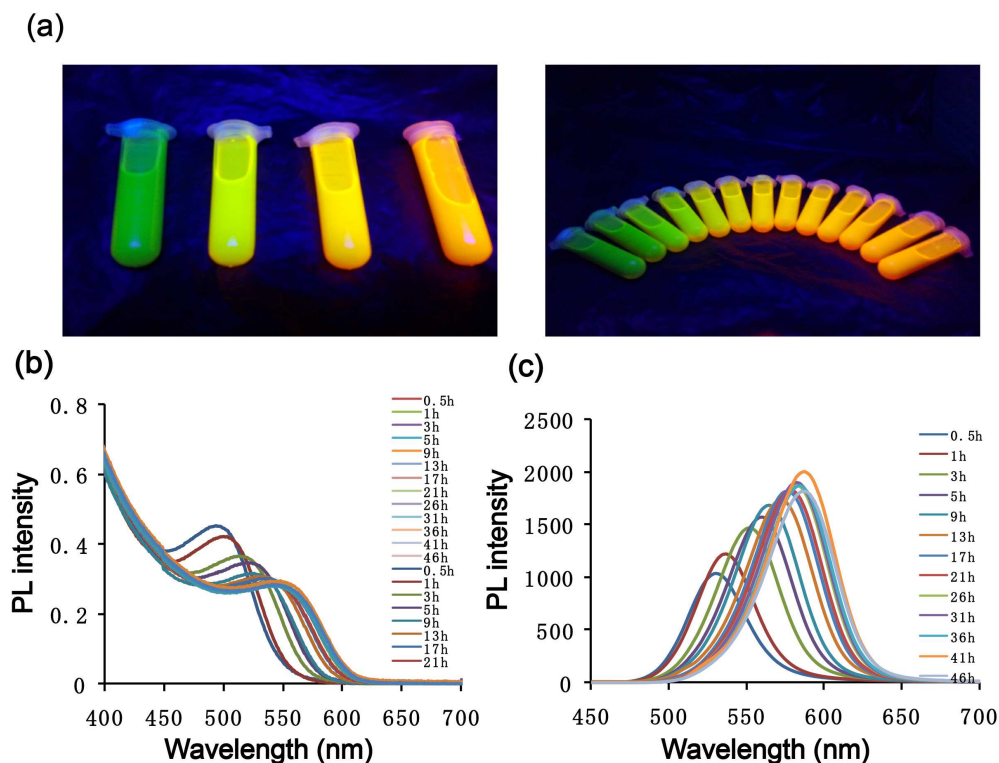


**Fig. 1** (a) UV light (365 nm) illumination of CdTe QDs with different sizes. (b) Absorption spectra of different reaction time of CdTe QDs aqueous solution. (c) Fluorescence emission spectra of different reaction time of CdTe QDs aqueous solution ( $\lambda_{ex} = 365$  nm)

caused the fluorescent quantum dot absorption spectra and fluorescence emission spectra red shift, which led to changes in the color of light-induced fluorescence. The red shift of the luminescence peaks of CdTe dispersion was also observed in another study to make CdTe luminescent nanowires, and the red shift occurred was also explained to be due to the decrease of confinement in one dimension associated with the quantum size effects<sup>29</sup>. The absorption peak maxima ranging from 494.0 nm to 551.0 nm, emission peaks ranging from 530.4 nm to 587.0 nm and the corresponding narrow FWHM (the full width at half maximum) of the band-edge luminescence was from 44 nm to 52 nm ( $\lambda_{ex}=365$  nm), which indicated the narrow size distribution of the as-prepared CdTe QDs<sup>30</sup>. The particle sizes and concentration of CdTe QDs were



calculated according to Peng's Eq.(1), Eq.(2) and Lambert–Beer's law Eq. (3) as shown in **Tab. 1**. Time dependent increase of the particle size of the forming QDs was observed, confirming the nanoparticles formation. At the end of the reaction, the particle size of the prepared QDs was 3.25 nm.

**Tab.1** Absorption and emission peak maxima, size and concentration of TGA-CdTe QDs in different refluxing time.

Time (h)	$\lambda_{max}$ (nm)	Em (nm)	PL intensity (fwhm)	PL (nm)	D (nm)	C (mol/L)
0.5	494.0	530.4	1042	44.0	2.17	1.32E-4
1	504.0	536.4	1226	44.6	2.45	9.66E-5
3	513.0	552.8	1469	48.1	2.66	7.59E-5
5	528.0	559.8	1568	49.0	2.95	5.81E-5
9	526.0	564.6	1687	49.4	2.92	5.57E-5
13	537.0	572.4	1736	51.0	3.08	4.90E-5
17	539.0	576.6	1821	51.0	3.11	4.77E-5
21	539.0	579.2	1831	51.1	3.11	4.61E-5
26	546.0	582.2	1885	51.4	3.20	4.40E-5
31	546.0	582.0	1899	52.1	3.20	4.31E-5
36	548.0	584.2	1866	51.3	3.22	4.12E-5
41	548.0	587.0	1999	51.4	3.22	4.38E-5
46	551.0	586.8	1821	52.4	3.25	4.17E-5

Then, highly fluorescent amino-functionalized core-shell CdTe@SiO<sub>2</sub> particles were prepared via the water-in-oil (W/O) reverse microemulsion method. Properly modifying the surface of the fluorescent nanoparticles with functionalized groups is important for their further applications. Therefore, (3-aminopropyl)trimethoxysilane (APS) was used as a standard silane coupling chemistry to graft primary amine groups to the surface of the silica nanoparticles<sup>31</sup>. As shown in **Fig. 2a**, the changing of the PL properties of the QDs was demonstrated in the coating process. After coating of the silica film, the PL peaks of the particles are blue shifted very slightly and the FWHM showed no obvious change, despite of the fluorescence intensity of the

nanoparticles decreases dramatically.

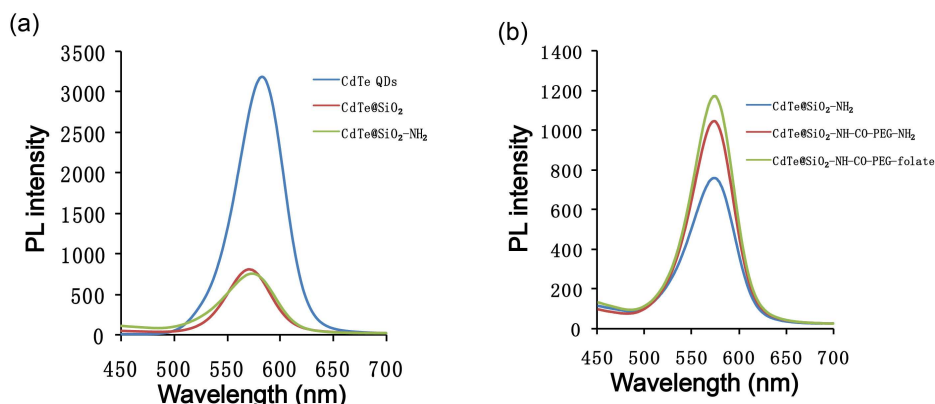


**Fig. 2.** (a) The fluorescence spectra of CdTe QDs, CdTe@SiO<sub>2</sub> and CdTe@SiO<sub>2</sub>-NH<sub>2</sub> dispersed in PBS solution. (b) The fluorescence spectra of CdTe@SiO<sub>2</sub>-NH<sub>2</sub>, CdTe@SiO<sub>2</sub>-NH-CO-PEG-NH<sub>2</sub> and CdTe@SiO<sub>2</sub>-NH-CO-PEG-folate nanoparticles dispersed in PBS. ( $\lambda_{ex}=365$  nm)

The prepared CdTe@SiO<sub>2</sub> particles were subjected to biofunctionalization using PEG moiety (PEG-Fol) through the use of amino groups to render biocompatibility and specificity for the luminescent nanomaterials. Both of the FR-targeted CdTe@SiO<sub>2</sub>-NH-CO-PEG-folate and non-targeted CdTe@SiO<sub>2</sub>-NH-CO-PEG-NH<sub>2</sub> fluorescent probes represent desirable optical properties, prepared by the reaction of CdTe@SiO<sub>2</sub>-NH<sub>2</sub> and NH<sub>2</sub>-PEG-COOH (or Folate-PEG-COOH). As shown in **Fig. 2b**, coating a long PEG chain on the surface of CdTe@SiO<sub>2</sub>-NH<sub>2</sub> nanoparticles would contribute to some increase of the fluorescence intensity without any PL peak shift, which means a lot for the bioapplications or further functionalizations of the nanoparticles.

The size and morphology of prepared nanoparticles were investigated using high-resolution TEM (HR-TEM). Samples (CdTe@SiO<sub>2</sub>, CdTe@SiO<sub>2</sub>-NH-CO-PEG-NH<sub>2</sub> and CdTe@SiO<sub>2</sub>-NH-CO-PEG-folate nanoparticles) were dropped in thin carbon film and dried under vacuum before the HR-TEM imaging. As shown in the TEM

micrographs in **Fig. 3**, the CdTe QDs ( $E_m = 587.0$  nm) perform nearly spherical, highly monodisperse, clear lattice lines, and average size about 3.3 nm, which is close to the calculated value (3.25 nm) showed in **Tab.1**.

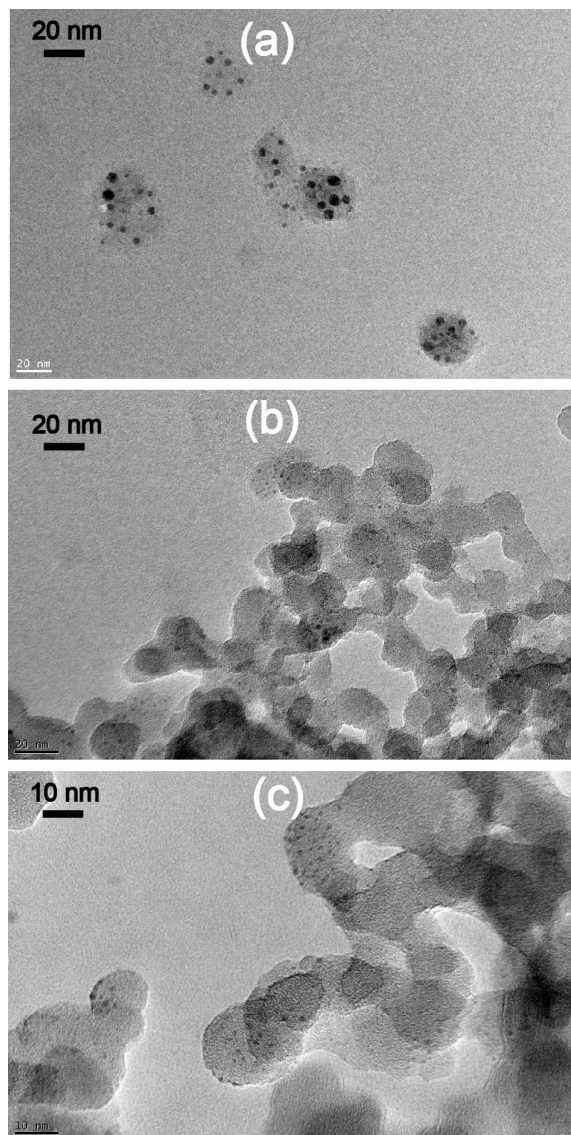


**Fig. 3.** HR-TEM images of the as-performed nanoparticles. **(a)** HR-TEM images of CdTe@SiO<sub>2</sub> nanoparticles. **(b)** HR-TEM images of CdTe@SiO<sub>2</sub>-NH-CO-PEG-NH<sub>2</sub> nanoparticles. **(c)** HR-TEM images of CdTe@SiO<sub>2</sub>-NH-CO-PEG-folate nanoparticles. The images also implied that the materials are highly mono-dispersed without any sign of particle aggregation. The silica coating and subsequently surface modifications was carried out successfully as evidenced by TEM. As shown in **Fig. 3**,

the TEM clearly demonstrated that multiple CdTe QDs are successfully embedded into silica shells which are nearly spherical in shape with an approximate average size of 25 nm. The images are also clearly showed that most of the CdTe@SiO<sub>2</sub> composite particles were separated from each other, while the CdTe@SiO<sub>2</sub>-NH<sub>2</sub> nanoparticles was clearly observed to be serious aggregation due to the surface charge changed. After modified with a long PEG chain, the aggregation situation has turned better to some extent as we expected , which also demonstrated the successful modification of PEG indirectly.

**Tab. 2** Surface charge of the prepared nanoparticles.

Nanoparticles	Zeta potential (mV)
CdTe QDs	-51.05
CdTe@SiO <sub>2</sub>	-47.97
CdTe@SiO <sub>2</sub> -NH <sub>2</sub>	7.25
CdTe@SiO <sub>2</sub> -NH-CO-PEG-NH <sub>2</sub>	8.06
CdTe@SiO <sub>2</sub> -NH-CO-PEG-folate	6.32

The zeta potentials of CdTe QDs, CdTe@SiO<sub>2</sub>, CdTe@SiO<sub>2</sub>-NH<sub>2</sub>, CdTe@SiO<sub>2</sub>-NH-CO-PEG-NH<sub>2</sub> and CdTe@SiO<sub>2</sub>-NH-CO-PEG-folate nanoparticles were -51.05 mV, -47.97mV, 7.25 mV, 8.06 mV and 6.32 mV, respectively as shown in **Tab. 2**. The negative potentials of CdTe and CdTe@SiO<sub>2</sub> particles were produced by the carboxyl groups of the capped TGA and surface silanol groups. After the modification to introduce the amine groups, the resulted CdTe@SiO<sub>2</sub>-NH<sub>2</sub>, CdTe@SiO<sub>2</sub>-NH-CO-PEG-NH<sub>2</sub> and CdTe@SiO<sub>2</sub>-NH-CO-PEG-folate nanoparticles turned out be low total positive charges. <sup>1</sup>H-NMR analysis showed principal peaks (in ppm) related to the folate moiety with the chemical shifts of 8.59 ppm(s), 7.60 ppm(d), 6.73 ppm(d), and the PEG moiety with the chemical shift of 3.65(m). MADLI-TOF

showed the molecular weight of  $\text{NH}_2\text{-PEG-COOH}$  ( $3600\pm 500$ ) and Folate-PEG-COOH ( $4000\pm 500$ ). These data suggest that folate was successfully attached to  $\text{NH}_2\text{-PEG-COOH}$ .

The presence of surface amino groups of the composite nanoparticles was further proved by the fluorometric assay of primary amines using fluorescamine<sup>32</sup>. The fluorescamine itself does not show fluorescence and does not have any fluorescent emission in acetone. However, when fluorescamine reacts with primary amines, the product has a maximum emission wavelength of 475 nm. As shown in **Fig. 4**, only when the solution contain both of fluorescamine and  $\text{CdTe@SiO}_2\text{-NH}_2$  nanoparticles, a new high-PL emission peak at 475 nm appears, which suggests that amine groups were successfully grafted on the surface of silica nanoparticles. The presence of amino groups lays a foundation for further conjugation with biological molecules.

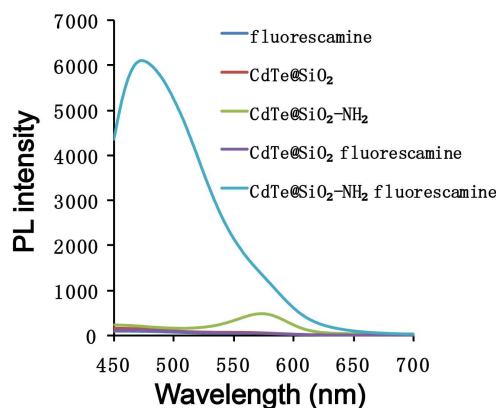


**Fig. 4.** Fluorescence spectra determination of amine groups on the surface of nanoparticles based on fluorescamine method. ( $\lambda_{\text{ex}}=365$  nm)

After months of storage at 4 °C in dark, the fluorescence emission spectrum of the CdTe QDs colloid solution and novel fluorescent probes of  $\text{CdTe@SiO}_2\text{-NH-CO-PEG-NH}_2$ ,  $\text{CdTe@SiO}_2\text{-NH-CO-PEG-folate}$  prepared in this study were investigated. As shown in **Fig. 5a** and **5b**, CdTe QDs remained nearly

unchanged luminescent properties, both of the PL peaks and FWHM of CdTe@SiO<sub>2</sub>-NH-CO-PEG-NH<sub>2</sub> and CdTe@SiO<sub>2</sub>-NH-CO-PEG-folate nanoparticles have a little blue shift of 5.0 nm and 8.0 nm respectively, compared to several months ago, which suggest good optical stability.

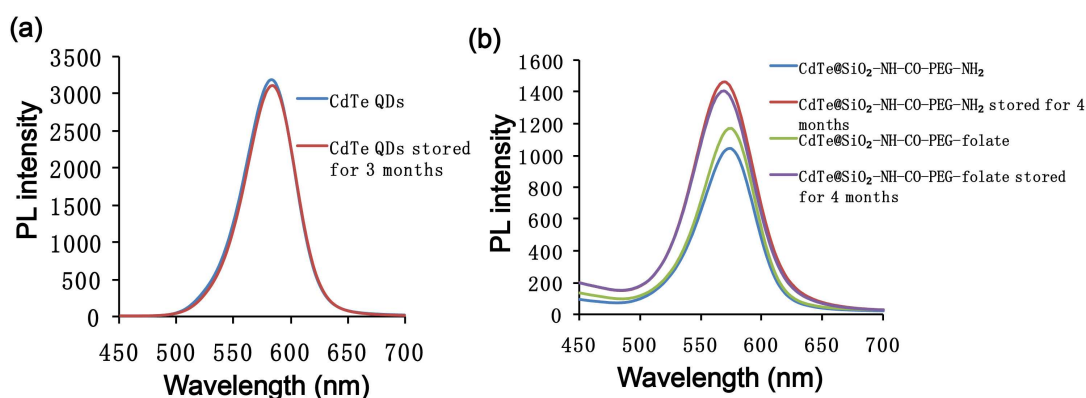


**Fig. 5.** (a) Fluorescence emission spectrum of CdTe QDs colloid solution after being stored for 3 months. (b) Fluorescence emission spectrum of CdTe@SiO<sub>2</sub>-NH-CO-PEG-NH<sub>2</sub> and CdTe@SiO<sub>2</sub>-NH-CO-PEG-folate nanoparticles after being stored for 4 months. The excitation wavelength is 365 nm.

### Cytotoxicity studies

Cytotoxicity of CdTe QDs, CdTe@SiO<sub>2</sub>-NH<sub>2</sub>, CdTe@SiO<sub>2</sub>-NH-CO-PEG-NH<sub>2</sub> and CdTe@SiO<sub>2</sub>-NH-CO-PEG-folate nanoparticles were evaluated in KB cells using an MTT assay. As shown in **Fig. 6**, the IC<sub>50</sub> value of FR-targeted fluorescent probe CdTe@SiO<sub>2</sub>-NH-CO-PEG-folate is about twice lower compared to non-targeted fluorescent probe CdTe@SiO<sub>2</sub>-NH-CO-PEG-NH<sub>2</sub>. The KB cells are FR-over expressed cells. The FR-targeting nanoparticles with folate ligand could be uptaken into KB cells via the carrier system, thus increasing the cell cytotoxicity. All of the silica coated and PEGylation nanoparticles have a much higher IC<sub>50</sub> value than that bare CdTe QDs. The results demonstrate that encapsulating a silica film and PEGylation on CdTe QDs significantly reduced the cytotoxicity of CdTe QDs and

folate molecules successfully play the role of targeting FR-positive cancer cells.

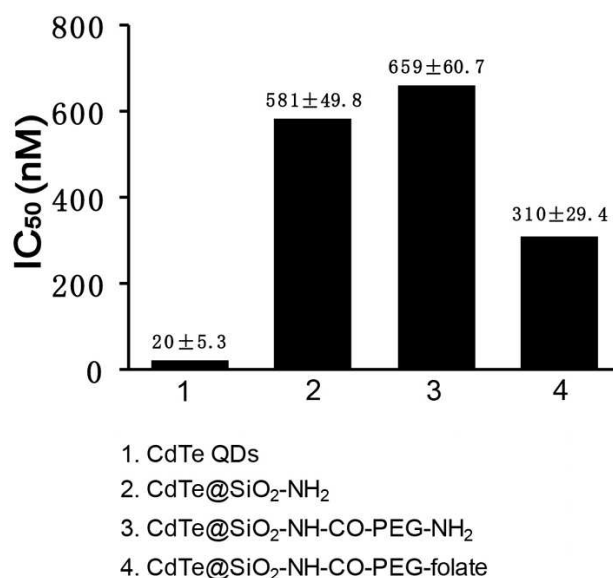


**Fig. 6.** The cytotoxicity of the fluorescent nanoparticles for KB cancer cells. Values shown are means and standard deviations (n=3)

#### Cellular uptake of the fluorescent probes

Uptake of FR-targeted CdTe@SiO<sub>2</sub>-NH-CO-PEG-folate and non-targeted CdTe@SiO<sub>2</sub>-NH-CO-PEG-NH<sub>2</sub> nanoparticles by KB cells were investigated by fluorescence microscopy and flow cytometry. As shown in **Fig. 7**, FR-targeted CdTe@SiO<sub>2</sub>-NH-CO-PEG-folate nanoparticles were more efficiently taken up by KB cells compared to non-targeted CdTe@SiO<sub>2</sub>-NH-CO-PEG-NH<sub>2</sub> nanoparticles, and the uptake could be blocked by 1mM free folic acid. Flow cytometry results showed that the mean fluorescence intensity of KB cells treated with FR-targeted CdTe@SiO<sub>2</sub>-NH-CO-PEG-folate was about 2.5 times of that treated with non-targeted CdTe@SiO<sub>2</sub>-NH-CO-PEG-NH<sub>2</sub> nanoparticles, and targeting effect can be blocked by free folic (shown in **Fig. 8.** and **Tab. 3**). These data show that FR-targeted CdTe@SiO<sub>2</sub>-NH-CO-PEG-folate fluorescent probes could effectively target the KB

cells through the FR.

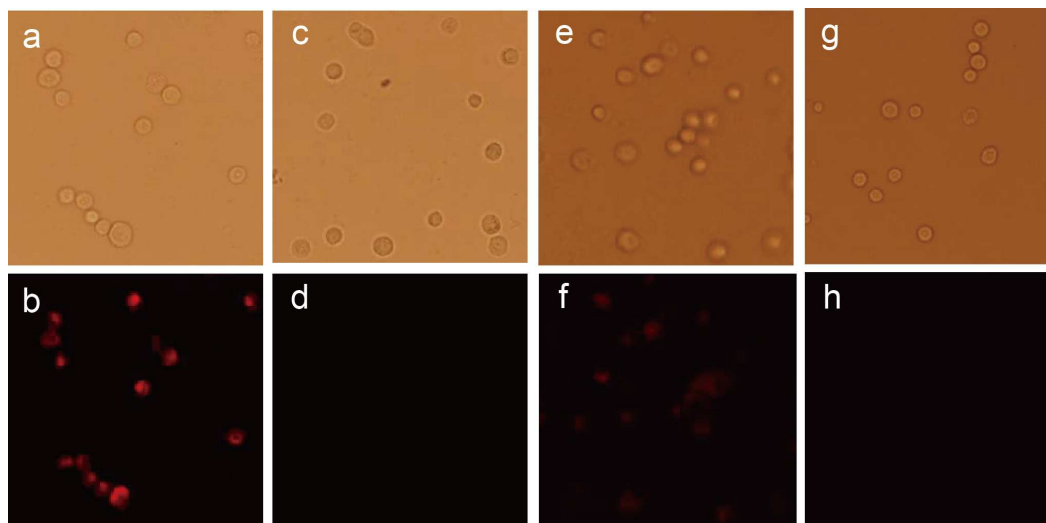


**Fig. 7.** The confocal imaging of CdTe@SiO<sub>2</sub>-NH-CO-PEG-folate and CdTe@SiO<sub>2</sub>-NH-CO-PEG-NH<sub>2</sub> fluorescent probes by KB cells under green light with an exposure time of 200 msec. Left panels cells were visualized in the fluorescence mode; right panels the same fields in the bright mode. Panels (a) and (b), cells were treated with CdTe@SiO<sub>2</sub>-NH-CO-PEG-folate nanoparticles; panels (c) and (d), cells were treated with CdTe@SiO<sub>2</sub>-NH-CO-PEG-NH<sub>2</sub> nanoparticles; panels (e) and (f), cells treated with CdTe@SiO<sub>2</sub>-NH-CO-PEG-folate nanoparticles plus 1mM free folate; panels (g) and (h), cells treated with PBS as control.

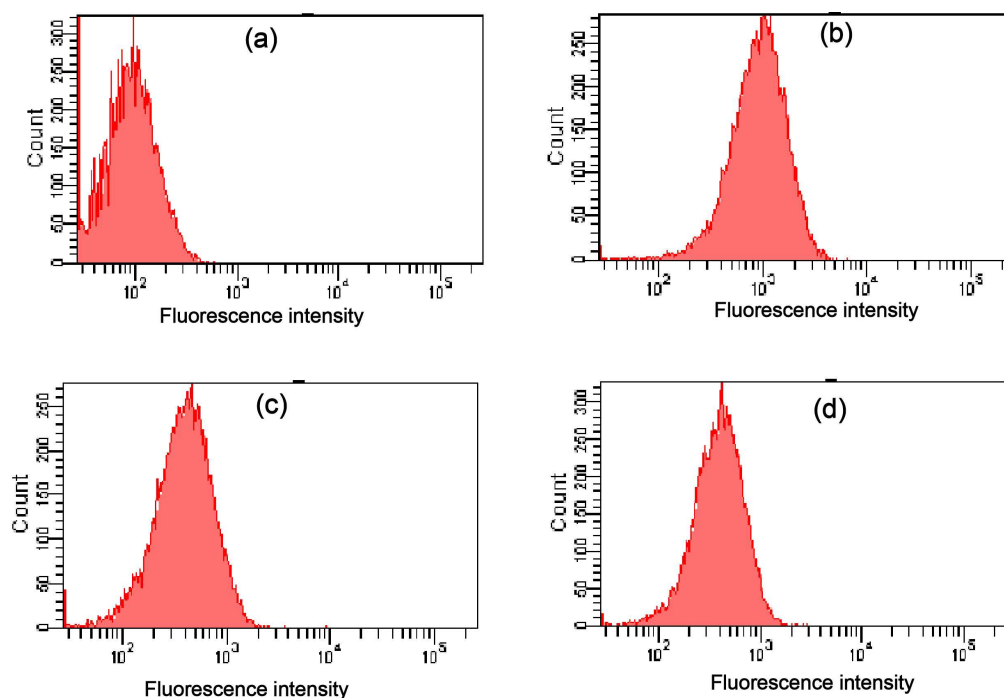


**Fig. 8.** Uptake of the prepared fluorescent probes by KB cells measured by flow



cytometry. (a) control; (b) CdTe@SiO<sub>2</sub>-NH-CO-PEG-folate; (c) CdTe@SiO<sub>2</sub>-NH-CO-PEG-NH<sub>2</sub>; (d) CdTe@SiO<sub>2</sub>-NH-CO-PEG-folate plus 1mM free folic.

**Tab. 3** The flow cytometry datas show relative uptake of the prepared fluorescent probes in KB cells.

Treatment group	%Parent	Fluorescence intensity
	Q1	Mean
CdTe@SiO <sub>2</sub> -NH-CO-PEG-folate	71.2	1050
CdTe@SiO <sub>2</sub> -NH-CO-PEG-NH <sub>2</sub>	27.7	438
CdTe@SiO <sub>2</sub> -NH-CO-PEG-folate plus 1mM free folic	28.6	454
PBS	0.5	97

The study demonstrated using silica shell over the QDs core was able to reduce metal ion leakage, and the biocompatibility was also achieved using PEG-folate biofunctionalization of CdTe QDs for biological applications, although the passivation shell may reduce the luminescent property of the QDs and also requires additional processing procedures. The CdTe@SiO<sub>2</sub>-NH-CO-PEG-folate was exhibited with good stable luminescence and biocompatible property. The added advantage of PEG-folate functionalized QDs gained the ODs into cells decently and effectively and helped the QDs endocytosed by cells within short period of time. From all the above results, we have concluded that PEG-folate biofunctionalized CdTe QDs showed increased biocompatibility and high specificity, which were essential strategies for utilization of materials for cancer imaging and diagnosis.

## CONCLUSIONS

In conclusion, based-on the aqueous CdTe QDs colloid nanocrystal strategy, we have prepared a kind of novel fluorescent probe with good stability, low cytotoxicity, satisfactory sensitivity and biocompatibility for effective tumor targeting *via* the folate receptor mediated endocytosis. Even after silica coating, surface amine group

modification and the novel folate ligand Folate-PEG-COOH functionalized, the nanoparticles remained excellent optical properties of parent QDs. The functionalized nanoparticles showed cell specific targeting through folate receptors and are internalized by folate mediated endocytosis. We believed that our luminescent nanoprobes would be promising for a much wider range of biological applications and early diagnosis of human cancer due to their superior properties. .

## EXPERIMENTAL

### Materials

Tellurium powder ( $\geq 99.99\%$ ) was obtained from Aladdin Chemistry Co., Ltd. (Shanghai, China).  $\text{NaBH}_4$  ( $\geq 96.0\%$ ) and  $\text{CdCl}_2 \cdot 2.5\text{H}_2\text{O}$  ( $\geq 99.0\%$ ) was purchased from Sinopharm Chemical Reagent Co., Ltd. (Beijing, China). Thioglycolic acid (TGA) ( $\geq 98\%$ ), Tetraethyl orthosilicate (TEOS) ( $\geq 99.999\%$ ), (3-Aminopropyl) trimethoxysilane (97%), Amino-polyethylene glycol (peg)-carboxyl ( $\text{NH}_2$ -PEG-CM, mw3400) were purchased from Sigma-Aldrich Chemical Co. (St. Louis, MO). Dicyclohexylcarbodiimide (DCC) and N-hydroxysuccinimide (NHS) were purchased from ACROS ORGANICS (Belgium). 1-ethyl-3-[3-dimethylamino propyl]carbodiimide hydrochloride (EDC) and folic acid ( $\geq 97\%$ ) were purchased from J&K Chemical Ltd. (Beijing, China). Ammonia aqueous solution (25 wt-28wt %), cyclohexane, n-hexanol, acetone, iso-propyl alcohol, ethanol, Dimethyl sulfoxide (DMSO) were purchased from Sinopharm Chemical Reagent Co., Ltd. (Beijing, China). Triethylamine was purchased from Shanghai Linfeng Chemical Reagent CO., LTD. (Shanghai, China). Fluorescamine (98%) was obtained from

Aladdin Reagent Co., Ltd. (Shanghai, China). KB cells were provided by Tongji Medical College (Huazhong University of Science and Technology, China). RPMI 1640 10×medium was purchased from Sigma-Aldrich Chemical Co. (St. Louis, MO). Fetal bovine serum (FBS) was purchased from Hangzhou Sijiqing Biological Engineering Materials Co., Ltd. (Hangzhou, China). L-Glutamine was obtained from Ling-Fei Technology (Wuhan, China). Trypsin and 3-(4,5-dimethylthiazol-2-yl)-2,5-diphenyltetrazolium bromide (MTT) were obtained from WuHan Goodtimebio-Technology Co., Ltd (Wuhan, China). Ultrapure water was used for the preparation of all solutions. All reagents and solvents were of analytical and were used without further purification.

### Preparations

**Sodium Hydrogen Telluride.** The sodium hydrogen telluride (NaHTe) was prepared using the reaction between tellurium powder and sodium borohydride (NaBH<sub>4</sub>) according to the previous published papers with slight modifications<sup>33</sup>. Briefly, ultrapure water (5 mL) was added to a three-necked flask connected to a Schlenk line and deaerated by N<sub>2</sub> for 15 min. After sodium borohydride (151.3 mg, 4 mmol) and tellurium powder (127.6 mg, 1 mmol) were added in the flask, the reaction was carried out at 40 °C with vigorous magnetic stirring. The whole process was purged with N<sub>2</sub>. After approximately 2 h, the reaction was chilled in an ice bath. Immediately, the white sodium tetraborate precipitation appeared in the flask.

**TGA-capped CdTe QDs.** Typically, the CdTe QDs were prepared in aqueous phase using the TGA as the stabilizing agent following the method described previously<sup>34</sup>.

Briefly, in a three-necked flask with a condenser attached,  $\text{CdCl}_2 \cdot 2.5\text{H}_2\text{O}$  (0.4567 g, 2 mmol) was dissolved in ultrapure water (100 mL), and TGA (334  $\mu\text{L}$ , 4.8 mmol) was added under stirring, followed by adjusting the pH to 8.2 by adding NaOH (1M) dropwise. The resulting solution was deaerated by  $\text{N}_2$  for 30 min. Under vigorous stirring, the fresh prepared colorless oxygen-free NaHTe solution (1 mmol) was injected through a syringe at room temperature. In our experiments, the typical molar ratio of  $\text{Cd}^{2+}$ : NaHTe: TGA was 1:0.5:2.4. The reaction mixture was heated to reflux (96°C) under  $\text{N}_2$  atmosphere for 2 h. Ultimately, the highly luminescent water-soluble CdTe QDs were obtained and stored at 4 °C in dark for further use.

The particle sizes and concentration of CdTe QDs were calculated according to Peng's Eq.(1), Eq.(2) and Lambert–Beer's law Eq. (3)<sup>35, 36</sup>

$$\text{Eq.(1) } D = (9.8127 \times 10^{-7})\lambda^3 - (1.7147 \times 10^{-3})\lambda^2 + (1.0064)\lambda - 194.84$$

$$\text{Eq.(2) } \varepsilon = 10043(D)^{2.12}$$

$$\text{Eq. (3) } A = \varepsilon cl$$

**CdTe@SiO<sub>2</sub> nanoparticles.** According to the previous investigation on silica coating of quantum dots, fluorescent CdTe@SiO<sub>2</sub> particles embedded multiple QDs were prepared via the water-in-oil reverse microemulsion method, with some modifications<sup>37</sup>. First, the crude CdTe QDs solution (160 $\mu\text{L}$ ) was mixed with alkaline solution containing 0.45wt % ammonia and  $15.9 \times 10^{-3}$  M NaOH (320  $\mu\text{L}$ ). Then, under vigorous stirring, the resultant mixture was introduced into a liquid system containing cyclohexane (7.5 mL), n-hexanol (1.8 mL), and Triton X-100 (1.77 mL). After 30 min, TEOS (100 $\mu\text{L}$ ) was introduced. Then, the reaction system was sealed and kept under

stirring in the dark at room temperature for 3 days. Acetone was used to terminate the reaction, and the resultant precipitate of CdTe@SiO<sub>2</sub> particles was subsequently washed in sequence with isopropanol, ethanol and water, respectively. During each washing procedure, the particle suspension was typically collected by centrifugation and then dispersed in the next solvent through supersonication. In the end, CdTe@SiO<sub>2</sub> dispersed in phosphate-buffered saline (PBS, pH7.2) were obtained and kept at 4 °C in dark for further use.

**CdTe@SiO<sub>2</sub>-NH<sub>2</sub> nanoparticles.** (3-Aminopropyl)trimethoxysilane (APS) (2 μL) was introduced into the reaction system for 3 days after the hydrolysis and condensation of TEOS for grafting amine groups on the surface of CdTe@SiO<sub>2</sub> particles. The reaction system was then kept under stirring in dark for one day. The post-processing were the same as those for CdTe@SiO<sub>2</sub> particles, thus the resultant CdTe@SiO<sub>2</sub>-NH<sub>2</sub> nanoparticles were obtained.

**Folate-PEG-COOH.** Folate-PEG-COOH was synthesized in organic phase. The solution of folic acid (6.5 mg) in DMSO (1 mL) was reacted with DCC (15.5 mg) and NHS (8.63 mg) at room temperature for 12 h. Then, amine-PEG-carboxy (NH<sub>2</sub>-PEG-CM) (42.5 mg) and triethylamine (50μL) were added to the above solution, and the reaction was allowed for 48 h at room temperature under magnetic stirring. The obtained Folate-PEG-carboxy was then purified by Sephadex G-25 gel-filtration chromatography and subsequently dried by lyophilization. A yellow powder product was obtained with a yield of 53.9%. The identity of the product was confirmed by <sup>1</sup>H NMR in D<sub>2</sub>O and MALDI-TOF.

**CdTe@SiO<sub>2</sub>-NH-CO-PEG-NH<sub>2</sub> and CdTe@SiO<sub>2</sub>-NH-CO-PEG-folate fluorescent probes.** The synthesis of CdTe@SiO<sub>2</sub>-NH-CO-PEG-NH<sub>2</sub> and CdTe@SiO<sub>2</sub>-NH-CO-PEG-folate fluorescent probes was described as follows. The CdTe@SiO<sub>2</sub>-NH<sub>2</sub> dispersion in PBS (1.8 ml) was added in a round-bottom flask. NH<sub>2</sub>-PEG-COOH (100μL) or Folate-PEG-COOH (1 mmol/L), EDC (50μL, 2 mmol/L) and NHS (50μL 4 mmol/L) were added subsequently under magnetic stirring. The reaction was stirred overnight at room temperature. The product CdTe@SiO<sub>2</sub>-NH-CO-PEG-NH<sub>2</sub> and CdTe@SiO<sub>2</sub>-NH-CO-PEG-folate were obtained *via* centrifugation at 10000 rpm for 15 min, and then washed with PBS for more than 3 times. The resultant fluorescent probes were re-dispersed in PBS and kept at 4 °C in dark.

### **Characterization**

UV-visible absorption spectra were measured using a 756-PC UV-visible spectrophotometer (Shanghai Spectrum Instrument Co., Ltd., Shanghai, China). Fluorescence experiments were performed using an F-4600 FL spectrometer (Hitachi high technologies corporation, Japan). A JEM-2100 High Resolution Transmission Electron Microscope (HR-TEM) (JEOL Ltd, Japan) was used to measure the size diameter and morphology of the nanoparticles at an accelerating voltage of 200 kV. The zeta potential of the nanoparticles was measured using a Multifunctional Zeta PALS Potential and Particle Size Analyzer (Brookhaven Instruments Corporation, NY). All samples were characterized directly at room temperature under ambient conditions.

### Cytotoxicity assay

KB cells were grown at 37 °C under 5% CO<sub>2</sub> in folate-free RPMI 1640 medium containing 10% FBS. KB cells with 6×10<sup>3</sup> cells/mL were seeded into 96 well plates and maintained 24 h in 100µL of the cell culture medium. These cells were divided into four groups which were named as CdTe QDs, CdTe@SiO<sub>2</sub>-NH<sub>2</sub>, CdTe@SiO<sub>2</sub>-NH-CO-PEG-NH<sub>2</sub> and CdTe@SiO<sub>2</sub>-NH-CO-PEG-folate and the negative control group. The same volume of nanoparticles PBS suspensions were added to each well of the corresponding group, respectively. The PBS was used as the negative control group. The plates were all incubated for 48 h at 37 °C. Then, the mixture in each well of four groups were washed with PBS once, and subsequently replaced with folic-free RPMI 1640 medium (200µL) and freshly prepared MTT (20µL, 5 mg/mL in PBS buffer with pH 7.2). The plate was incubated for 4 h at 37 °C. After removing the solution, the cells were lysed by adding 150µL methyl sulfoxide. The 96-well plate was gently shaken for 10 min, and then the absorbance of the produced purple formazan at 490 nm was monitored using a ELISA reader (Thermo Labsystems; Shanghai Co.Ltd., Vantaa, Finland).

### Fluorescence microscopy

Briefly treated with trypsin, cells were suspended with folic-free and FBS-free RPMI 1640 medium. KB cell suspension with a proper concentration were divided into four groups, incubated with the same volume and same concentration of FR-targeted CdTe@SiO<sub>2</sub>-NH-CO-PEG-folate, non-targeted CdTe@SiO<sub>2</sub>-NH-CO-PEG-NH<sub>2</sub>, FR blocking group containing 1mM free folic acid and negative control

PBS group respectively for 1 h at 37 °C under 5% CO<sub>2</sub>. After incubation, the cells were washed two times with ice-cold PBS to remove unbound nanoparticles by centrifugation at 1500 rpm for 5 min. Ultimately, the cells were re-suspended in 300µL PBS and drop on glass slides for confocal imaging through an Olympus 1×71 inverted fluorescence microscopy to determine the uptake of FR-targeted and non-targeted fluorescent probes by KB cells.

### **Flow cytometry analysis**

Four groups of KB cell suspensions were prepared and carried out the subsequent procedure described as the 2.7.2. The final 300µL cell suspensions were detected by flow cytometry (BD-LSR II) with an excitation filter of 488 nm.

### **Acknowledgement**

This research was partially supported by National Natural Science Foundation of China (NSFC) (No.81072596 , No.81301235) and the Key Program of Natural Science Foundation of Hubei Province, China (2011CDA029).

### **Bibliographic references and notes**

1. A. Jemal, F. Bray, M. M. Center, J. Ferlay, E. Ward and D. Forman, CA: A Cancer Journal for Clinicians, 2011, 61, 69-90.
2. M. D. Guimaraes and R. Chojniak, AJR Am J Roentgenol, 2013, 201, W919.
3. T. Hussain and Q. T. Nguyen, Adv Drug Deliv Rev, 2013.
4. M. Fang, J. P. Yuan, C. W. Peng, D. W. Pang and Y. Li, Biomaterials, 2013, 34, 8708-8717.
5. A. C. O'Farrell, S. D. Shnyder, G. Marston, P. L. Coletta and J. H. Gill, Br J Pharmacol, 2013, 169, 719-735.
6. R. Di Corato, N. C. Bigall, A. Ragusa, D. Dorfs, A. Genovese, R. Marotta, L. Manna and T. Pellegrino, ACS Nano, 2011, 5, 1109-1121.



7. A. C. Poulouse, S. Veerananarayanan, M. S. Mohamed, S. Raveendran, Y. Nagaoka, Y. Yoshida, T. Maekawa and D. S. Kumar, *J Fluoresc*, 2012, 22, 931-944.
8. M. Cheki, M. Moslehi and M. Assadi, *Eur Rev Med Pharmacol Sci*, 2013, 17, 1141-1148.
9. M. S. Murahari and M. C. Yergeri, *Curr Pharm Des*, 2013, 19, 4622-4640.
10. S. Santra and A. Malhotra, *Wiley Interdiscip Rev Nanomed Nanobiotechnol*, 2011.
11. U. Resch-Genger, M. Grabolle, S. Cavaliere-Jaricot, R. Nitschke and T. Nann, *Nat Methods*, 2008, 5, 763-775.
12. C. B. Murray, D. J. Norris and M. G. Bawendi, *Journal of the American Chemical Society*, 1993, 115, 8706-8715.
13. X. Peng, L. Manna, W. Yang, J. Wickham, E. Scher, A. Kadavanich and A. P. Alivisatos, *Nature*, 2000, 404, 59-61.
14. W. C. Law, K. T. Yong, I. Roy, H. Ding, R. Hu, W. Zhao and P. N. Prasad, *Small*, 2009, 5, 1302-1310.
15. Y. Lu, Y. Zhong, J. Wang, Y. Su, F. Peng, Y. Zhou, X. Jiang and Y. He, *Nanotechnology*, 2013, 24, 135101.
16. A. M. Derfus, W. C. W. Chan and S. N. Bhatia, *Nano Letters*, 2003, 4, 11-18.
17. R. Bakalova, Z. Zhelev, I. Aoki, K. Masamoto, M. Mileva, T. Obata, M. Higuchi, V. Gadjeva and I. Kanno, *Bioconjug Chem*, 2008, 19, 1135-1142.
18. S. T. Selvan, C. Li, M. Ando and N. Murase, *Chemistry Letters*, 2004, 33, 434-435.
19. T. Nann and P. Mulvaney, *Angew Chem Int Ed Engl*, 2004, 43, 5393-5396.
20. W. Stöber, A. Fink and E. Bohn, *Journal of Colloid and Interface Science*, 1968, 26, 62-69.
21. S.-Y. Chang, L. Liu and S. A. Asher, *Journal of the American Chemical Society*, 1994, 116, 6739-6744.
22. J. Song, Z. Dai, W. Guo, Y. Li, W. Wang, N. Li and J. Wei, *J Nanosci Nanotechnol*, 2013, 13, 6924-6927.
23. S. Tong, S. Hou, B. Ren, Z. Zheng and G. Bao, *Nano Lett*, 2011, 11, 3720-3726.
24. N. Abdullah Al, J. E. Lee, I. In, H. Lee, K. D. Lee, J. H. Jeong and S. Y. Park, *Mol Pharm*, 2013, 10, 3736-3744.
25. J. Gao, K. Chen, Z. Miao, G. Ren, X. Chen, S. S. Gambhir and Z. Cheng, *Biomaterials*, 2011, 32, 2141-2148.
26. Y. Zhao, S. Liu, Y. Li, W. Jiang, Y. Chang, S. Pan, X. Fang, Y. A. Wang and J. Wang, *J Colloid Interface Sci*, 2010, 350, 44-50.
27. W. T. Al-Jamal, K. T. Al-Jamal, B. Tian, A. Cakebread, J. M. Halket and K. Kostarelos, *Mol Pharm*, 2009, 6, 520-530.
28. J. Qian, K. T. Yong, I. Roy, T. Y. Ohulchanskyy, E. J. Bergey, H. H. Lee, K. M. Trampusch, S. He, A. Maitra and P. N. Prasad, *J Phys Chem B*, 2007, 111, 6969-6972.
29. Z. Tang, N. A. Kotov and M. Giersig, *Science*, 2002, 297, 237-240.
30. W.-h. Yang, W.-w. Li, H.-j. Dou and K. Sun, *Materials Letters*, 2008, 62, 2564-2566.
31. G. Wang, C. Wang, W. Dou, Q. Ma, P. Yuan and X. Su, *Journal of Fluorescence*,

2009, 19, 939-946.

32. S. De Bernardo, M. Weigele, V. Toome, K. Manhart, W. Leimgruber, P. Böhlen, S. Stein and S. Udenfriend, Archives of Biochemistry and Biophysics, 1974, 163, 390-399.

33. L. Y. Zhang, H. Z. Zheng, Y. J. Long, C. Z. Huang, J. Y. Hao and D. B. Zhou, Talanta, 2011, 83, 1716-1720.

34. M. A. Jhonsi and R. Renganathan, J Colloid Interface Sci, 2010, 344, 596-602.

35. W. W. Yu, L. Qu, W. Guo and X. Peng, Chemistry of Materials, 2003, 15, 2854-2860.

36. W. Guo, J. J. Li, Y. A. Wang and X. Peng, Journal of the American Chemical Society, 2003, 125, 3901-3909.

37. L. Jing, C. Yang, R. Qiao, M. Niu, M. Du, D. Wang and M. Gao, Chemistry of Materials, 2009, 22, 420-427.

### Table of Contents Graphic

CdTe@SiO<sub>2</sub>-NH-CO-PEG-folate nanoparticles were successfully prepared and it demonstrated tumor cell specific targeting through folate receptors via folate mediated endocytosis.

